A Digital Interferometric Array with Active Noise Illumination for Millimeter-Wave Imaging at 13.7 fps

Stavros Vakalis[1] and Jeffrey A. Nanzer[2]
Electrical and Computer Engineering, Michigan State University, USA
[1]vakaliss@msu.edu [2]nanzer@msu.edu

***Abstract*— We present millimeter-wave imagery at 13.7 frames-per-second (fps) using a digital 16-element interferometric antenna array operating at 37 GHz. The scene is illuminated incoherently using three low-cost noise transmitters, mimicking the properties of thermal radiation. The array is based on commercial components and 3D-printed horn antennas. The system architecture is presented, along with the signal processing algorithm, and real-time imaging results.**

***Keywords*— Millimeter-wave imaging, computational imaging, digital antenna arrays, distributed arrays, noise radar.**

I. Introduction

The use of microwave and millimeter-wave systems to generate images has been attracting increased interest recently due to the large number of applications that can benefit from imaging in bands outside of optical and infrared bands. Applications include contraband detection, non-destructive testing, remote sensing, search and rescue operations, and medical imaging, among others [1]–[4]. Additionally, microwave and millimeter-wave components are becoming increasingly cost efficient and widely available. Compared to the more commonly used optical frequencies, an important advantage of using microwave and millimeter-wave signals for image reconstruction is the fact that such signals can easily pass through clothing, fog, rain, and walls. Creating real-time imagery in millimeter-wave frequencies is more challenging than in optical frequencies due to the fact that most microwave and millimeter-wave imaging techniques require electrical or mechanical scanning of an aperture over the desired field of view, and are thus limited by the scanning speed. Computational imaging techniques can achieve staring operation, but with the cost of longer processing time [5], [6]. Passive millimeter-wave imagers can take advantage of the ambient thermal radiation and achieve real-time operation, however they require very high sensitivity at microwave and millimeter-wave frequencies, which results in high cost [7].

The capability of generating microwave imagery using incoherent signal transmission from noise sources in combination with an interferometric array was demonstrated in [8]. This approach eliminates the high sensitivity requirement of passive millimeter-wave systems by using active illumination and therefore much higher signal-to-noise ratio (SNR). However, only measurements using a small set of antennas moved to synthesize an array were shown and therefore video-rate image reconstruction was not demonstrated. This paper presents the design of a 16-element fully active digital 37 GHz incoherent imaging array with active noise illumination. The system provides millimeter-wave image reconstructions at 13.7 fps; this includes all latencies for the data acquisition time, the signal processing time, and the time for starting and stopping the data acquisition. This paper describes the hardware architecture and image reconstruction algorithm, and presents time-lapse images of the video-rate output.

II. Interferometric Imaging with Noise Sources

An interferometric antenna array captures the mutual coherence of electromagnetic radiation by cross-correlating its element responses pairwise. The response $\left\langle V_i(t)V_j^*(t)\right\rangle$ corresponds to the cross-correlation of the voltage response at the antenna element i and antenna element j respectively. The cross-correlations can be implemented using analog hardware with mixing capabilities or digitally by multiplying and integrating. Different antenna baselines correspond to different numbers of spatial fringes, which can be mapped to different points in the spatial frequency domain. By cross-correlating pairwise the response of different antenna elements, a large enough sample of the spatial frequency distribution of the scene can be obtained, which in radio astronomy is referred to as visibility $\mathcal{V}$, which is the 2-D Fourier transform of the scene intensity. The sampled visibility $\mathcal{V}_s$ can give the reconstructed scene intensity I_r through an inverse Fourier transform

$$I_r(\alpha,\beta) = \sum_{n}^{N}\sum_{m}^{M}\mathcal{V}_s(u_n,v_m)e^{j2\pi(u_n\alpha+v_m\beta)} \tag{1}$$

where $\alpha = \sin\theta\cos\phi$ and $\beta = \sin\theta\sin\phi$ are the direction cosines along the azimuth and elevation planes.

Interferometric imaging was first developed in radio astronomy, where large antenna arrays were observing the thermally generated electromagnetic radiation of galactic objects. More recently, passive millimeter-wave imagers have demonstrated that this technique can create imagery from thermal emissions of humans and other objects. However, both radio astronomy arrays and passive millimeter-wave arrays need to have highly sensitive receivers because thermal radiation at microwave and millimeter-wave frequencies has extremely low power. The reason that these systems need to be passive, is that the radiation from the scene needs to be spatio-temporally incoherent. This derives from the Van-Cittert Zernike theorem [9], [10], and can be interpreted as each point's response being sufficiently independent

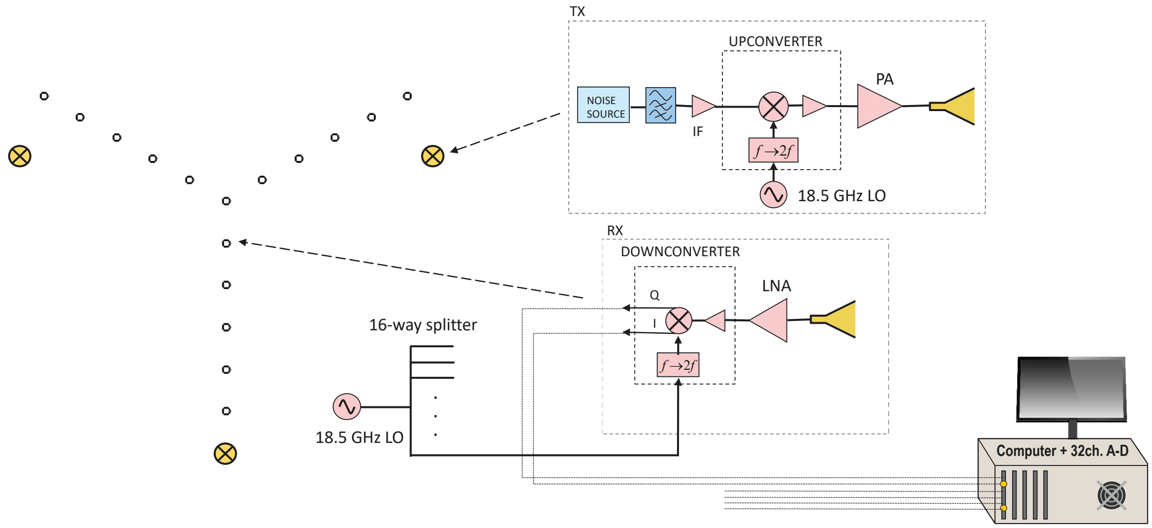

Fig. 1. 16-element active incoherent imaging system. 16 receivers (represented by white circles) are located in the locations of a Y-array and 3 transmitters are used (represented by the yellow circles with the crosses). The 16 receive waveforms are quadrature downconverted resulting in 32 waveforms captured by two 16-channel digitizers hosted in a computer.

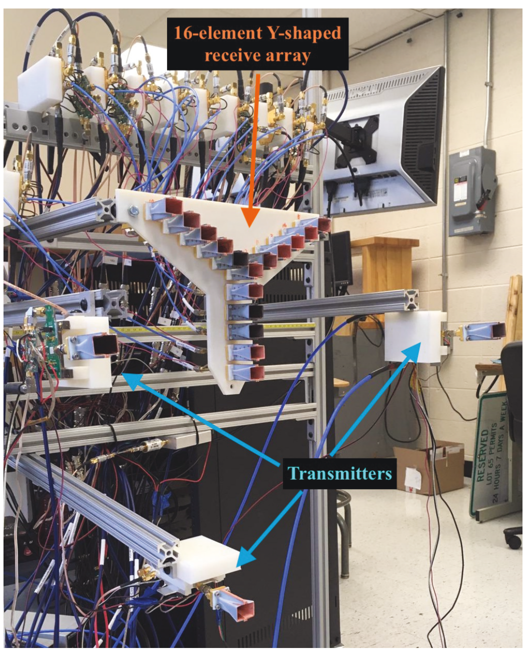

Fig. 2. Photograph of the active incoherent imaging system with 16 receivers and 3 transmitters.

from the others. The incoherence requirement is satisfied, when observing the random thermal emissions from stars, humans or other objects. However, in the case of traditional active systems, there is significant spatial correlation in the transmitted radiation, and therefore interferometric image reconstruction cannot successfully take place.

It was suggested in [8] that noise transmission from multiple locations could illuminate the scene in a spatio-temporally incoherent way mimicking thermal radiation, and therefore interferometric image reconstruction could feasibly be implemented. The active illumination can mitigate the high sensitivity requirements and reduce bandwidth and integration time by one order magnitude or more, when compared to passive millimeter-wave systems. This makes real-time millimeter-wave imagery much easier and more affordable using sparse arrays that are resistant to failures [11], [12]. Additionally, there is no need for beam scanning or computationally expensive algorithms. In this work, the first real-time video-rate imaging system based on active incoherent signal illumination and interferometric imaging is demonstrated.

III. Digital Millimeter-wave Array Architecture

The overall array architecture can be seen in Fig. 1. The 16 receivers are represented by white circles in Y-shape formation, a layout that provides a dense spatial frequency sampling function [13], and the 3 transmitters are represented by yellow circles with crosses. The operating frequency was 37 GHz. The distance between neighboring receive antenna elements was 24 mm (2.96 λ). The transmitters (shown at the top right) were three 0.2-2000 MHz low-cost baseband noise sources. For a flatter noise response over the band of interest, a high pass filter with a cutoff frequency of 20 MHz was used after each noise source, followed by a low-cost baseband amplifier of 30 dB gain and subsequently feeding to the intermediate frequency (IF) port of each upconverter. Three GaAs MMIC I/Q upconverters (Analog Devices HMC6787ALC5A), integrated with a frequency doubler for the local oscillator (LO) and a conversion gain of 10 dB, were used to mix the baseband noise to 37 GHz with an LO of 18.5 GHz. The three 37 GHz noise signals were then fed into three Analog Devices HMC7229LS6 power amplifiers, achieving approximately -10 dBm of noise power at 37 GHz.

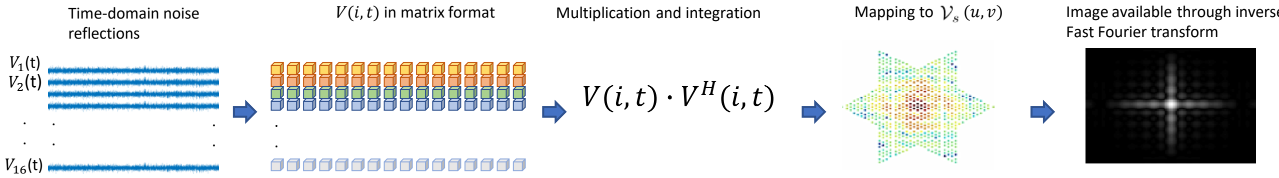

Fig. 3. Digital signal processing algorithm used in this paper. The reflected noise signals from the scene are captured in time domain and create the voltage matrix $V(i,t)$. The voltage matrix is multiplied with its conjugate transpose $V^H(i,t)$, which is a simple matrix multiplications and highly optimized. Afterwards they are mapped to spatial frequency samples and the image is available through an inverse fast Fourier transform.

For the 16 receivers, the schematic of which are shown below the transmitter schematic, each antenna was connected to a 20 dB gain Analog Devices HMC1040LP3CE low-noise amplifier (LNA) before being downconverted to baseband using 37-44 GHz GaAs MMIC I/Q downconverters (Analog Devices HMC6789BLC5A). The LO was distributed for the 16 receivers with two 8-way Mini-Circuits ZN8PD-02183-S+ splitters. The downconverted signals, both in-phase (I) and quadrature (Q) were captured using two 16-channel ATS9416 14 bit, 100 MS/s, AlazarTech waveform digitizers installed on a computer in master-slave mode. All the signal processing took place in MATLAB in real time.

A photograph of the imager can be seen in Fig. 2. A 3-D printed structure with vertical and horizontal dimension of 23 cm and 28 cm was used to hold the 16 receive antennas in the correct positions. The three transmitters were separated at a larger separation than the largest antenna baseline, in order to constructively and destructively interfere at a finer spatial variation than the resolution of the array and satisfy the incoherence requirement. Because the transmit pattern of the noise illumination is not required to be known in general, there is significant freedom in the transmitter placement. The antennas used in this implementation are 3-D printed standard gain 15 dBi horn antennas connected to WR-28 waveguide to 2.9 mm adapters. The 3-D printed horns were designed in ANSYS High Frequency Structure Simulator (HFSS) and were printed using VeroWhitePlus material on Stratus Objet Connex 350 Multi Material 3-D Printing System. For metallization, the structure was sputtered, first with a 60 nm Titanium for adhesion between copper and structure followed by 500 nm copper. After this step, the sputtered structure is electroplated with copper to achieve a thickness of 5-6 μm.

IV. Image Reconstruction Signal Processing

The signal processing algorithm is an important aspect of this system because the millimeter-wave array is element-level digital, and therefore it can significantly affect the image reconstruction time. The use of active illumination has increased the sensitivity of the system, and therefore decreased the integration time and bandwidth compared to passive systems. This is significant because the image formation algorithms can be run quickly in time-domain using multi-channel digitizers and a computer, without the need for dedicated processing hardware. Additionally, this system does not need any iterative algorithm to run for a large number of iterations, nor computationally expensive matrix inversion which is used in many inverse problems in electromagnetic imaging.

The image reconstruction process is summarized in Fig. 3. The incoherent noise reflections from the scene are captured in the time-domain from the 16 receivers and digitized using two 16-channel digitizers, capturing both their I and Q information. The $V_i(t)$ time-domain waveforms are complex and i refers to the $i-$th antenna element. They are stored in the complex voltage matrix $V(i,t)$ where i corresponds to the rows of the matrix, while t corresponds to the columns of the matrix. In order to do the cross-correlations between all the antenna elements in the array, which in this case is element-by-element multiplications and integration, we multiply $V(i,t)$ with its conjugate transpose $V^H(i,t)$. In this way each row of matrix $V(i,t)$, which is the $i-$th element complex response, will be multiplied with each column of $V^H(j,t)$, which is the conjugate response of the $j-$th element, and then summed (integrated). Afterwards the cross-correlations are mapped to visibility samples $\mathcal{V}_s$ and the image is available through an inverse fast Fourier transform (IFFT). At the right end of Fig. 3, the simulated reconstruction of a cross-shaped target is shown.

The resulting algorithm is fast and can produce video rate imaging at 13.7 fps, while the signal processing takes place on a computer with Intel i9-9820x processor; commonly in interferometric imaging systems such processing is implemented using a dedicated field-programmable gate array (FPGA). With an integration time of 20 μs and a sample rate of 100 Ms/s, the total time that it takes to transfer the data from the two data acquisition cards in matrix form in MATLAB is 54 ms because of the time lost in the communication between the digitizers and MATLAB. The signal processing algorithm is based on matrix multiplications and IFFTs, consuming only 2.3 ms of processing time, however plotting the image reconstruction consumes an additional 16.6 ms. Although a large amount of the total reconstruction time is spent on starting and stopping the data acquisition, the reconstruction is fast and smooth, at 13.7 fps and rarely found in 2-D snapshot electromagnetic imaging.

V. Real-Time Imaging Experiments

Experimental image reconstructions took place in a semi-enclosed environment with a person walking across the

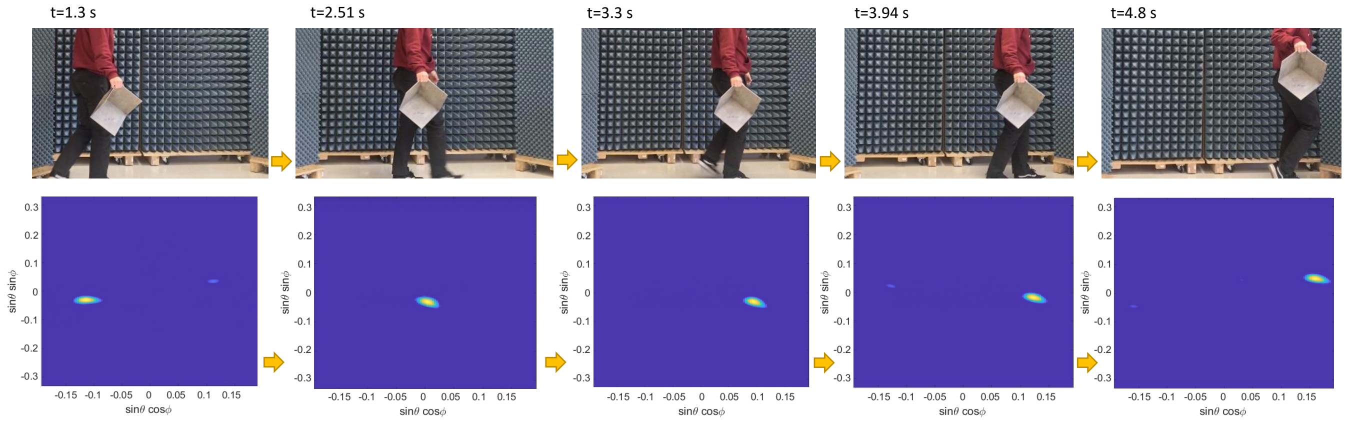

Fig. 4. Timelapse of a person walking in front of the imager at a distance of 3.3 m while holding a corner reflector at different time instances (top). Snapshots of real-time millimeter-wave image reconstructions of the corner reflector at 13.7 fps. (bottom).

field of view of the imager at a distance of 3.3 m away from the imaging array while holding a 20 dBsm corner reflector. A time lapse of the experimental measurements is shown in Fig. 4 where at the top part of the image snapshots show a person walking by while holding the corner reflector and at the bottom of Fig. 4 the video-rate millimeter-wave reconstructions can be seen. From left to right the snapshots correspond to timings of t=1.3 s, t=2.51 s, t=3.3 s, t=3.94 s, and t=4.8 s. The reconstructions at the bottom of Fig. 4 are not consecutive frames, and are meant to show the video-rate capabilities of the system over an extended time; the real-time image reconstruction rate is much faster, at 13.7 fps. At the last picture from the right, the walking person lifts up the corner reflector to show that the imager can track well displacements on the elevation plane. The dynamic range of the image has been optimized to reduce clutter and unwanted reflections from the semianechoic environment to a normalized ratio of [0.6,1]. The point response can be clearly seen and matches the target location.

VI. Conclusion

The first video-rate millimeter-wave imager based on active illumination using incoherent noise signals and a staring element-level digital interferometric receiver has been presented in this work. The active noise illumination enables higher SNR than passive systems, providing imagery with short integration times and fast image reconstruction. The overall hardware architecture is simple with no customized components, and the signal processing algorithm is computationally inexpensive with matrix multiplications and fast Fourier processing. The imaging system can produce image reconstructions at 13.7 fps, and can accurately reconstruct in real-time the response of a moving target at walking speed. This concept has the potential to significantly improve a number of millimeter-wave imaging applications. One such example is security screening, which poses a significant bottleneck throughout the airport security process. The fact that the architecture is simple and digital provides additional freedom for networked and distributed real-time millimeter-wave imaging systems, where larger arrays can be synthesized for improved imaging and sensing capabilities.

Acknowledgment

The authors would like to thank Brian Wright, Michigan State University, for help with the experimental setup.

References

[1] D. M. Sheen, D. L. McMakin, and T. E. Hall, "Three-dimensional millimeter-wave imaging for concealed weapon detection," *IEEE Trans. Microw. Theory Tech.*, vol. 49, no. 9, pp. 1581–1592, Sep 2001.

[2] J. A. Nanzer, "A review of microwave wireless techniques for human presence detection and classification," *IEEE Trans. Microw. Theory Tech.*, vol. 65, no. 5, pp. 1780–1794, May 2017.

[3] P. M. Meaney, M. W. Fanning, Dun Li, S. P. Poplack, and K. D. Paulsen, "A clinical prototype for active microwave imaging of the breast," *IEEE Trans. Microw. Theory Tech.*, vol. 48, no. 11, pp. 1841–1853, Nov 2000.

[4] P. C. Dubois, J. van Zyl, and T. Engman, "Measuring soil moisture with imaging radars," *IEEE Trans. Geosci. Remote Sens.*, vol. 33, no. 4, pp. 915–926, July 1995.

[5] T. Fromenteze, O. Yurduseven, J. Gollub, C. Decroze, D. Carsenat, and D. R. Smith, "Computational imaging using a mode-mixing cavity at microwave frequencies," *Appl. Phys. Lett.*, vol. 106, no. 19, May 2015.

[6] O. Yurduseven, V. R. Gowda, J. N. Gollub, and D. R. Smith, "Printed aperiodic cavity for computational and microwave imaging," *IEEE Microw. Wireless Compon. Lett.*, vol. 26, no. 5, pp. 367–369, May 2016.

[7] L. Yujiri, M. Schoucri, and P. Moffa, "Passive millimeter-wave imaging," *IEEE Microw. Mag.*, vol. 4, pp. 39–50, 2003.

[8] S. Vakalis and J. A. Nanzer, "Microwave imaging using noise signals," *IEEE Trans. Microw. Theory Tech.*, vol. 66, no. 12, pp. 5842–5851, Dec 2018.

[9] A. R. Thompson, J. M. Moran, and G. W. Swenson, *Interferometry and Synthesis in Radio Astronomy*. John Wiley and Sons, 2001.

[10] M. Born and E. Wolf, *Principles of optics*. Cambridge Univ. Pr., 1999.

[11] S. Vakalis and J. A. Nanzer, "Analysis of element failures in active incoherent microwave imaging arrays using noise signals," *IEEE Microw. Wireless Compon. Lett.*, vol. 29, no. 2, pp. 161–163, Feb 2019.

[12] ——, "Analysis of array sparsity in active incoherent microwave imaging," *IEEE Geosci. Remote Sens. Lett.*, vol. 17, no. 1, pp. 57–61, Jan 2020.

[13] A. Camps, J. Bara, I. C. Sanahuja, and F. Torres, "The processing of hexagonally sampled signals with standard rectangular techniques: application to 2-d large aperture synthesis interferometric radiometers," *IEEE Trans. Geosci. Remote Sens.*, vol. 35, no. 1, pp. 183–190, Jan 1997.